

# Weak Antiferromagnetic Order in Anisotropic Quantum Pyrochlores

Valeri N. Kotov

Department of Physics, Boston University, 590 Commonwealth Avenue, Boston, Massachusetts 02215

We study the ground state properties of an anisotropic, quasi-2D version of the quantum ( $S=1/2$ ) pyrochlore antiferromagnet. In the presence of Dzyaloshinsky-Moriya interactions, in addition to the Heisenberg exchanges, it is shown that two types of ordered magnetic states are generally possible: non coplanar “chiral,” and coplanar antiferromagnetic order. The magnetic moments in all cases are determined by the Dzyaloshinsky-Moriya interactions and in this sense the antiferromagnetic order is “weak.”

## I. INTRODUCTION AND DESCRIPTION OF THE MODEL

The pyrochlore antiferromagnet is strongly frustrated and the structure of its ground state represents a challenging problem in the field of magnetism. It has been argued that, for purely Heisenberg interactions, both the classical and quantum versions of the model are magnetically disordered.<sup>1,2,3</sup> It also appears that in the extreme quantum limit ( $S=1/2$ ), lattice-symmetry breaking and spontaneous dimerization take place, although the ground state still exhibits macroscopic degeneracy.<sup>3,4,5</sup> Thus it is natural to expect that interactions beyond the Heisenberg exchange, as well as inclusion of various magnetic anisotropies, can impose their own order, such as orbital, dimer, or magnetic, or combinations of these. Effects due to orbital degeneracy,<sup>6</sup> long-range dipolar interactions,<sup>7</sup> and spin-lattice interactions<sup>8</sup> have been studied. Ising anisotropies can lead to the formation of “spin ice”,<sup>9</sup> which bears resemblance to the problem of proton disorder in ice.<sup>10</sup> Various planar<sup>11,12</sup> and other anisotropic<sup>13</sup> versions are also of strong theoretical interest, although they do not necessarily reflect the physics of the full 3D pyrochlore structure. Finally, under certain conditions, even more exotic ground states have been proposed, such as  $U(1)$  spin liquids,<sup>14</sup> or non-magnetic chiral states.<sup>15</sup>

In this work we will discuss certain aspects of the mechanism for magnetic order formation due to the presence of Dzyaloshinsky-Moriya (DM) interactions.<sup>16</sup> For the case of classical spins, this mechanism was studied recently<sup>17</sup> (see also<sup>18</sup>). The quantum case ( $S=1/2$ ) was discussed<sup>19</sup> within a technical scheme, similar to the one used in Ref. 3 for the pure Heisenberg case. A puzzling difference between the classical and the extreme quantum case is that in the classical case non planar, chiral-like (see below) as well as coplanar spin order is possible,<sup>17</sup> while in the quantum case only the chiral order was predicted.<sup>19</sup> Naturally, the way spin order emerges is also quite different in the classical and quantum cases, and for  $S=1/2$  the induced antiferromagnetic order is “weak,” in a sense that the ordered moment is proportional to the DM interaction itself. We point out that the role of DM interactions has been extensively studied only in the context of non-frustrated lattices, such as the square lattice, where it typically leads to weak ferromagnetic moments (present, for example, in the copper oxide compounds.) In frustrated lattices, however, the DM interaction effects can be much more profound, and are expected to lead to complex types of order.<sup>20</sup>

We consider the anisotropic version of the 3D pyrochlore lattice (Fig. 1(a)), where it can be viewed as weakly-coupled

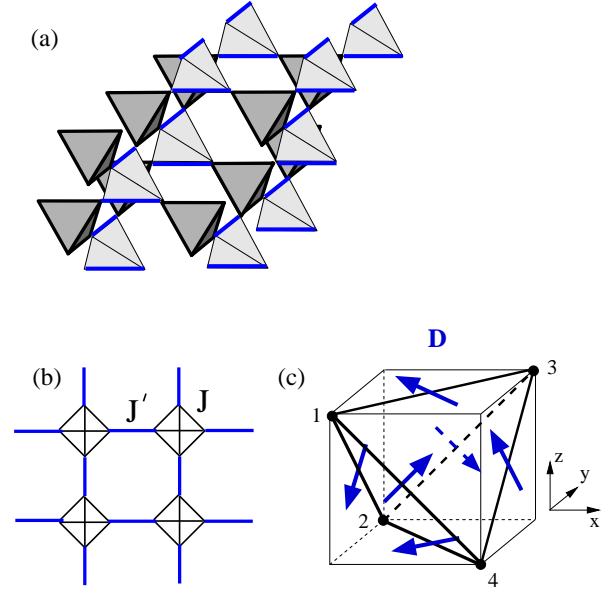


FIG. 1: (Color online) (a) Pyrochlore lattice (not all tetrahedra shown, for clarity.) (b) 2D Pyrochlore “layer,” showing the bonds in a (001) slice of the pyrochlore lattice. (c) DM interactions on a tetrahedron. The DM vectors are represented by blue arrows.

“layers,” defined in Fig. 1(b). Our goal is to investigate the possible types of magnetic order arising in this situation. It is technically very advantageous to consider the anisotropic limit, namely  $J_{\perp} \ll J' \ll J$ , where  $J_{\perp}$  is the Heisenberg exchange between the layers (thin black lines in Fig. 1(a)), and  $J'$  is the inter-tetrahedral exchange (solid blue lines in Fig. 1(a,b)).  $J$  is the exchange on the “strong” (shaded) tetrahedra, shown as plaquettes in Fig. 1(b). This strong-coupling approach is similar to the one used earlier,<sup>3,4,19</sup> except that now we consider an anisotropic version of it. The quasi 2D version allows us also to monitor the low-energy excitation spectrum, and determine the conditions under which different types of DM-induced order can arise. In order to implement this program we need to know the exact excitation spectrum on a single tetrahedron, which we calculate below, and then consider the lattice version of coupled tetrahedra. The lattice shown on Fig. 1(b) is a frustrated one, and we will present arguments why the strong-coupling expansion, governed by the parameter  $J' < J$ , should work well in determining the ground state structure. In order to avoid cumbersome formulas we present below results for the strict limit  $J_{\perp} = 0$ ,

while we have checked that the types of order we find are pretty generic (as long as the system is away from the strictly isotropic 3D case, which requires different considerations.) Notice also that the lattice of Fig. 1(b) is not the same as the 2D projection of the 3D pyrochlore, i.e. the checkerboard lattice,<sup>11</sup> which has valence-bond solid order (expected, quite generally, to compete with DM-induced magnetic order.)

The Hamiltonian reads

$$\mathcal{H} = \sum_{i,j} J_{i,j} \mathbf{S}_i \cdot \mathbf{S}_j + \sum_{i,j} \mathbf{D}_{i,j} \cdot (\mathbf{S}_i \times \mathbf{S}_j), \quad (1)$$

where the couplings  $J_{i,j}$  are assumed to be antiferromagnetic ( $J_{i,j} > 0$ ) and are distributed as already discussed. All spins are  $S=1/2$ . The DM vectors  $\mathbf{D}_{i,j}$  on a tetrahedron are shown in Fig. 1(c),<sup>17</sup> and have equal magnitude  $|\mathbf{D}_{i,j}| = |D|$ . Two patterns are possible: the one shown on the figure, and a pattern with all DM vectors reversed,  $\mathbf{D}_{i,j} \rightarrow -\mathbf{D}_{i,j}$ . There is no reason to expect that the induced order in the two cases will be the same; in fact two different types of order were found in the classical version.<sup>17</sup>

In the rest of the paper, we first calculate the exact spectrum on a single tetrahedron (Section II), which is then used to analyze the spectrum on the lattice and determine the possible types of order in Section III. Section IV contains our conclusions.

## II. QUANTUM SPINS ON A TETRAHEDRON WITH DM INTERACTIONS

Without DM interactions, the ground state on a tetrahedron of spins  $S=1/2$  is a twofold degenerate singlet. We denote the two states by  $|s_1\rangle, |s_2\rangle$ . Their explicit definition is given in Appendix A. The spectrum above the ground state consists of 3 degenerate triplets ( $|p_\alpha\rangle, |q_\alpha\rangle, |t_\alpha\rangle$ ,  $\alpha = x, y, z$ ), see Appendix A, as well as  $S=2$  states which are irrelevant for our purposes. However, the DM interactions break spin-rotational symmetry, and thus lead to mixing of singlet and triplet states. The ground state is still degenerate, and the two new ground states are:

$$\begin{aligned} |\Psi\rangle &= \alpha |s_2\rangle \\ &+ \frac{i\beta}{\sqrt{3}} \left\{ |p_x\rangle + |p_y\rangle + |q_x\rangle - |q_y\rangle + 2\sqrt{2}|t_z\rangle \right\}, \\ |\Phi\rangle &= \alpha |s_1\rangle + i\beta (|p_x\rangle - |p_y\rangle + |q_x\rangle + |q_y\rangle). \end{aligned} \quad (2)$$

From now on we measure all energies in units of  $J$ , i.e. we set  $J = 1$ , and consequently  $J'/J \rightarrow J'$ ,  $D/J \rightarrow D$ , etc. The ground state energy, corresponding to the states (2) is

$$E_0 = -1 + \frac{\sqrt{2}}{4} D - \frac{1}{4} \left[ 4 + 4\sqrt{2}D + 26D^2 \right]^{1/2}. \quad (3)$$

For small  $D \ll 1$ ,

$$E_0 \approx -\frac{3}{2} - \frac{3}{2} D^2. \quad (4)$$

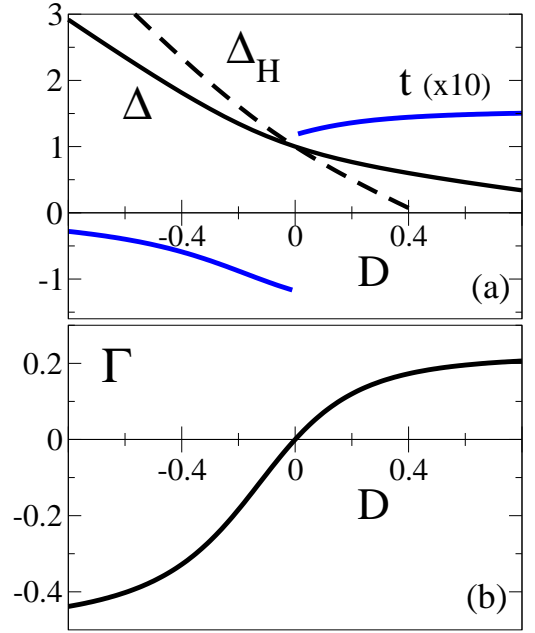


FIG. 2: (Color online) (a) The gaps  $\Delta = E_b - E_0$  (solid line),  $\Delta_H = E_b(H) - E_0$  (dashed line), and the “hopping” parameter  $t$  (Eq. (18)), solid blue line, as a function of the DM interaction strength. (b) The parameter  $\Gamma$  (Eq. (15)) which determines the magnitude of the ordered moments.  $D$  is in units of  $J = 1$ .

The coefficients  $\alpha, \beta$  in the wave-functions (2) are given explicitly by the formulas

$$\alpha = \frac{A}{\sqrt{A^2 + 4}}, \quad \beta = \frac{\alpha}{A}, \quad A \equiv -\frac{\sqrt{6}D}{3/2 + E_0}. \quad (5)$$

It is also useful to have the expansion for small  $D$ ,

$$A \approx \frac{2\sqrt{6}}{3} \frac{1}{D}, \quad \alpha \approx \text{sign}(D), \quad \beta \approx \frac{3}{2\sqrt{6}} |D|. \quad (6)$$

In our convention, the positive sign of  $D$ ,  $D > 0$  in all the above equations corresponds to the pattern shown in Fig. 1(c) (called “indirect” in Ref. 17), while  $D < 0$  (“direct” case from Ref. 17) is the situation when all arrows in Fig. 1(c) are reversed.  $|D|$  is the magnitude of the  $\mathbf{D}_{i,j}$  vectors.

Next, the first excited state (which we call  $|b\rangle$ ) is

$$|b\rangle = \frac{1}{\sqrt{6}} \left\{ |p_x\rangle + |p_y\rangle + |q_x\rangle - |q_y\rangle - \sqrt{2}|t_z\rangle \right\}, \quad (7)$$

with the exact energy

$$E_b = -\frac{1}{2} - \sqrt{2}D. \quad (8)$$

The next excited state is the “triplet”  $|\mathbf{P}\rangle$  with components:

$$|P_z\rangle = \frac{1}{2} \left\{ -|p_x\rangle + |p_y\rangle + |q_x\rangle + |q_y\rangle \right\}, \quad (9)$$

$$|P_{x,y}\rangle = \frac{1}{2} \left\{ |p_z\rangle \pm |q_z\rangle + \sqrt{2}|t_{x,y}\rangle \right\}. \quad (10)$$

The corresponding energy is

$$E_{\mathbf{P}} = -\frac{1}{2} - \frac{\sqrt{2}}{2}D. \quad (11)$$

For  $D = 0$  all excited states are degenerate and separated by an energy gap  $J = 1$  from the ground state. However for finite  $D$ , the  $b$ -state is the lowest (for  $D > 0$ ), and the variation of its gap  $\Delta = E_b - E_0$  as a function of  $D$  is shown in Fig. 2(a). In fact the gap vanishes for the (unphysically) large value of  $D = \sqrt{2}$ ; on the other hand the gap increases for  $D < 0$ . We proceed to explore if this difference can affect the type of magnetic order on the lattice (i.e. we study the conditions under which  $b$  can condense.)

### III. LOW-ENERGY EFFECTIVE LATTICE THEORY: CHIRAL VERSUS COPLANAR SPIN ORDER

#### A. Low-energy dynamics of interacting spins

The ground state structure from (2) implies that the spin operators have non-zero matrix elements of the type  $\langle \Psi | \mathbf{S}_i | \Phi \rangle$ . This is due to the presence of triplet states within the ground state subspace. Using the explicit form for the various triplet-triplet transition matrix elements, summarized in (A1), we obtain

$$\mathbf{S}_i = \Gamma \Lambda_i T_i^y, \quad (12)$$

where the vectors  $\Lambda_i$  are defined as

$$\begin{aligned} \Lambda_1 &= (-1, -1, 1), & \Lambda_2 &= (-1, 1, -1), \\ \Lambda_3 &= (1, 1, 1), & \Lambda_4 &= (1, -1, -1). \end{aligned} \quad (13)$$

The site label  $i = 1, 2, 3, 4$  in  $\mathbf{S}_i$ ,  $\Lambda_i$ , refers to the numbering of spins on a tetrahedron as displayed in Fig. 1(c). The operator  $T_i^y$  is defined as (its bold index  $\mathbf{i}$  refers to the whole tetrahedron)

$$T_i^y = \frac{i}{2} (\Psi^\dagger \Phi - \Phi^\dagger \Psi), \quad (14)$$

where  $\Psi^\dagger, \Phi^\dagger$  are operators that create the two ground states. Obviously  $T^y$  is the  $y$  (“magnetic”) component of the pseudospin operator  $\mathbf{T} = 1/2$ , defined in such a way that  $T^z = \pm 1/2$  label the two ground states (2), i.e.  $T^z = \frac{1}{2}(\Phi^\dagger \Phi - \Psi^\dagger \Psi)$ . The coefficient  $\Gamma$  in (12) depends on  $D$  through the wave-function coefficients,

$$\Gamma = \frac{4}{3} \alpha \beta - \frac{2}{\sqrt{3}} \beta^2 \approx \frac{2}{\sqrt{6}} D, \quad (D \ll 1). \quad (15)$$

We have also given the small  $D$  expansion which follows from (6). The plot of the exact function  $\Gamma = \Gamma(D)$  is shown in Fig. 2(b); notice that it is not  $D \rightarrow -D$  symmetric.

In the lattice geometry of Fig. 1(b), the effective interaction between the pseudospins is determined by the spin-spin interactions, and appears already at order  $J'$ . From (12) we easily obtain

$$\hat{\mathcal{H}}_{\text{eff}}^{(DM)} = -J'\Gamma^2 \sum_{\langle ij \rangle} T_i^y T_j^y, \quad (16)$$

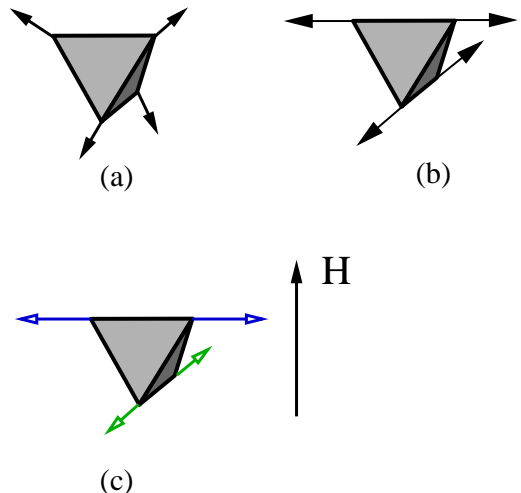


FIG. 3: (Color online) Types of magnetic order: (a) Chiral, (b) Coplanar, and (c) Coplanar in an external magnetic field (blue arrows are longer than green ones.)

implying that ferromagnetic ordering takes place (since  $J' > 0$ ), i.e. on every tetrahedron  $\langle T_i^y \rangle = 1/2$  (or  $\langle T_i^y \rangle = -1/2$ ). The Ising symmetry  $T_i^y \rightarrow -T_i^y$  is spontaneously broken. Physically, the state  $\langle T_i^y \rangle = 1/2$  corresponds to a unique ground state formed as the linear combination:  $(|\Phi\rangle + i|\Psi\rangle)/\sqrt{2}$ . There is magnetic order in this ground state, as follows from (12):  $\langle \mathbf{S}_i \rangle = (1/2)\Gamma\Lambda_i$ ; it is shown in Fig. 3(a). This is a magnetic “chiral” state, characterized by a non-zero scalar chirality  $\langle \mathbf{S}_i \cdot (\mathbf{S}_j \times \mathbf{S}_k) \rangle \neq 0$ . The magnitude of the magnetic moment is  $|\langle \mathbf{S}_i \rangle| = (\sqrt{3}/2)|\Gamma|$ , and the order is “weak” in a sense that  $\Gamma$  is determined by the value of the DM vectors. It is interesting to note that chiral order has been discussed in the context of spin liquid physics,<sup>15,21</sup> where one can presumably have a state with broken time-reversal symmetry and yet not magnetic order. In our case however the presence of DM interactions (which break spin-rotation symmetry) makes any time-reversal broken state magnetic.

Magnetic chiral spin states were also discussed in the context of the full 3D pyrochlore lattice and in other (quasi 2D) non-frustrated situations.<sup>19,22</sup> Such states generally compete with dimer order, which technically manifests itself in the presence of  $T_i^x, T_i^z$  operators in the effective Hamiltonian. Averages of such operators in the ground state lead to dimer order, and in turn diminish the magnetic,  $T_i^y$  component.<sup>3,19,22</sup> The specifics of this competition depend on the lattice. In our case (Fig. 1(b)) the issue of spontaneous dimerization has not been studied, to the best of our knowledge. However, it is clear that couplings involving  $T_i^x, T_i^z$  appear only in order  $(J')^4$ , and higher. Thus we will assume they can be neglected in the limit  $J' \ll 1$ . Given the coefficient in (16), a more precise criterion for the magnetic order to be dominant over potential spontaneous dimerization is  $J'\Gamma^2 > (J')^4$ , which we implicitly assume to be satisfied. Thus (16) determines the ground state structure within the degenerate subspace, and the degeneracy is lifted as explained previously, by locking  $\langle T_i^y \rangle = 1/2$ , which will be assumed from now on. (The choice

$\langle T_i^y \rangle = -1/2$  leads to time-reversal of all magnetic states.)

Now we write the effective Hamiltonian for the lowest excited state  $b$ , Eq. (7). It is convenient to express the spin operators in the ground state  $\langle T_i^y \rangle = 1/2$  via the  $b, b^\dagger$  operators, similarly to the way it is summarized for the case of zero chirality ( $D = 0$ ) in (A1). Performing the necessary calculations, we obtain

$$\begin{aligned} S_{1,3}^x &= \pm \frac{t}{\sqrt{2}} (1 - i\sqrt{3}) b^\dagger + \text{h.c.}, & S_{2,4}^x &= S_{1,3}^x, \\ S_{1,3}^y &= \pm \frac{t}{\sqrt{2}} (1 + i\sqrt{3}) b^\dagger + \text{h.c.}, & S_{2,4}^y &= -S_{1,3}^y, \\ S_{1,3}^z &= \sqrt{2}tb^\dagger + \text{h.c.}, & S_{2,4}^z &= -S_{1,3}^z. \end{aligned} \quad (17)$$

In (17) we use notation such that the lower left index of  $S_{i,j}^\alpha$  (which stands for either  $S_i^\alpha$  or  $S_j^\alpha$ ) corresponds to the upper sign on the right hand side, and the lower right index—to the lower sign (i.e.  $S_1^x = +\frac{t}{\sqrt{2}}(1 - i\sqrt{3})b^\dagger + \text{h.c.}$ , and  $S_3^x = -\frac{t}{\sqrt{2}}(1 - i\sqrt{3})b^\dagger + \text{h.c.}$ , etc.) The formulas (17) refer to a single tetrahedron which we label (as before) with a bold index  $\mathbf{i}$  (i.e.  $b$  will carry this index,  $b \rightarrow b_{\mathbf{i}}$ ). The site index  $i = 1, 2, 3, 4$  of the spins  $S_i^\alpha$  on a tetrahedron again follows the convention shown in Fig. 1(c). We also emphasize that equations (12),(17) simply mean that the spin operators have the same matrix elements as the right hand sides of those equations, i.e. the expressions should be added up to obtain the total spin operators.

The coefficient  $t$  is defined as

$$t \equiv \frac{\alpha}{6\sqrt{2}} + \frac{\beta}{2\sqrt{6}} \approx \frac{\text{sign}(D)}{6\sqrt{2}} + \frac{|D|}{8}, \quad (D \ll 1), \quad (18)$$

and the small  $D$  limit expansion is also given. Figure 2(a) shows a plot of  $t$ .

The effective Hamiltonian, describing the low-energy dynamics of  $b$  can now be readily obtained:

$$\begin{aligned} H_b &= \Delta \sum_{\mathbf{i}} b_{\mathbf{i}}^\dagger b_{\mathbf{i}} + \sum_{\langle ij \rangle} (t_1 b_{\mathbf{i}}^\dagger b_{\mathbf{j}} + t_2 b_{\mathbf{i}}^\dagger b_{\mathbf{j}}^\dagger + \text{h.c.}) \\ &+ t_3 \sum_{\mathbf{i}} (b_{\mathbf{i}}^\dagger + b_{\mathbf{i}}). \end{aligned} \quad (19)$$

The parameters appearing in  $H_b$  are

$$\begin{aligned} \Delta &= E_b - E_0, \\ t_1 &= -2t^2(J' + \sqrt{2}D'), \\ t_2 &= 4t^2(J' - \sqrt{2}D'/2), \\ t_3 &= 4 \left( \frac{\Gamma}{2} \right) t(2\sqrt{2}J' + D'). \end{aligned} \quad (20)$$

Here we have also included the DM interactions  $D'$  which appear on inter-tetrahedral bonds (and we set  $D' = D$  from now on); their distribution is explained in Ref. 17. The presence of  $D'$  is not qualitatively (or even quantitatively) important for our following discussion. The quantity  $\Delta$  is the on-site gap already discussed previously, while  $t_1, t_2$  originate from the representation (17) for two spins on neighboring tetrahedra (thus  $t_1, t_2 \sim J't^2$ ). Finally,  $t_3 \sim J't\Gamma$  reflects terms of

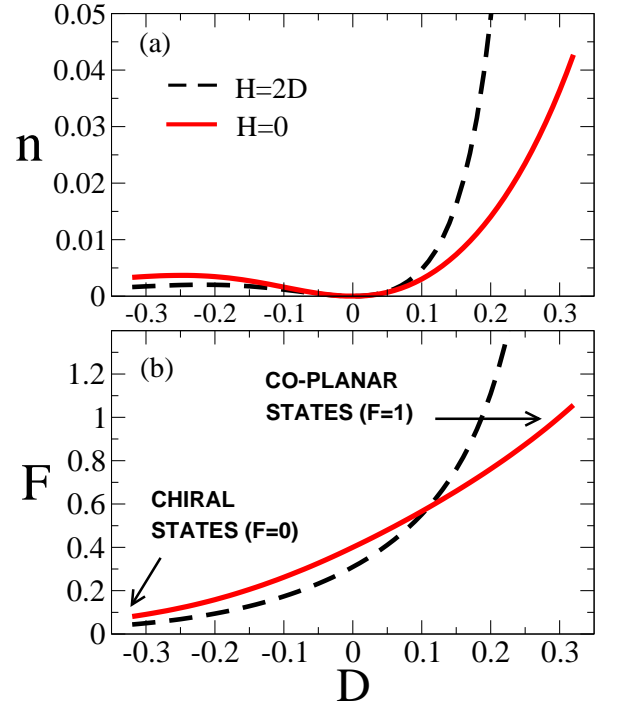


FIG. 4: (Color online) (a) The  $b$  condensate density  $n = |\langle b \rangle|^2$  in zero field (solid red line), and in a finite magnetic field (dashed line). (b) The parameter  $F$  characterizing the level of coplanarity of the spin order at zero field (solid red line) and in a finite magnetic field along [001] (dashed line.)

the type  $T_i^y (b_{\mathbf{i}}^\dagger + \text{h.c.})$ , i.e. the coupling between the magnetic component of the ground state pseudospin and the magnetic excited state (we have set  $T_i^y \rightarrow \langle T_i^y \rangle = 1/2$ , as (16) demands.)

From (19) it follows that  $b$  condenses with a condensate value of

$$\langle b_{\mathbf{i}} \rangle = \langle b \rangle = -\frac{t_3}{\Delta + 4(t_1 + t_2)}, \quad (21)$$

calculated in the mean-field approximation. It is easy to check that  $\langle b \rangle < 0$ . The  $b$  bosons are hard-core, in order to represent correctly the original spin operators. However their hard-core nature can be neglected, and thus the mean-field works well, as long as the condensate density  $n = |\langle b \rangle|^2$  is small. We find this to be the case for  $|D| \lesssim 0.4$ ; beyond this value the boson repulsion would stabilize the rise of  $\langle b \rangle$ , but this regime occurs only for unphysically large values of  $D$ . The density  $n$  is plotted in Fig. 4(a) with a solid red line, and from now on we set  $J' = J$ , for definitiveness. It is clear that a big difference exists between the two cases  $D > 0$  and  $D < 0$ , partially reflecting the difference in the behavior of  $\Delta$  (Fig. 2(a)). For  $D > 0$  the value of  $\langle b \rangle$  is significantly different from zero, while  $\langle b \rangle \approx 0$  for  $D < 0$ .

Let us now investigate how the presence of  $\langle b \rangle \neq 0$  affects the spin order in the ground state. We combine equations (12) and (17), with  $T_i^y = 1/2$ ,  $b = \langle b \rangle$ , to obtain (the site index  $i$

is defined as in Fig. 1(c)

$$\begin{aligned} \langle S_i^z \rangle &= (-1)^{i+1} \frac{\Gamma}{2} (1 - F), \quad i = 1, 2, 3, 4, \\ \langle S_1^x \rangle &= \langle S_2^x \rangle = -\langle S_3^x \rangle = -\langle S_4^x \rangle = -\frac{\Gamma}{2} \left( 1 + \frac{F}{2} \right), \\ \langle S_1^y \rangle &= \langle S_4^y \rangle = -\langle S_3^y \rangle = -\langle S_2^y \rangle = -\frac{\Gamma}{2} \left( 1 + \frac{F}{2} \right), \end{aligned} \quad (22)$$

where we have defined

$$F = -\frac{4\sqrt{2}t}{\Gamma} \langle b \rangle = \frac{4\sqrt{2}t}{\Gamma} |\langle b \rangle|. \quad (23)$$

The function  $F$  is plotted in Fig. 4(b)(solid red line.) For  $F = 0$  the magnetic order is of the chiral type (Fig. 3(a)), while for  $F = 1$  it is coplanar, as shown in Fig. 3(b). At the coplanar point the magnetic moment is  $|\langle \mathbf{S}_i \rangle| = (3\sqrt{2}/4)\Gamma$ . For an intermediate value of  $F$  the order is not coplanar. We find the universal trend that for  $D < 0$  the order is almost chiral ( $F$  is small), and for  $D > 0$  there is a strong tendency towards coplanar order.

### B. Enhancement of coplanar order by magnetic field

We now proceed to investigate how an external magnetic field can affect the ordering tendencies described above. It is known, for example in dimer systems,<sup>23</sup> that a field can induce magnetization perpendicular to it in the presence of DM interactions. The exact solution of the problem in our case is rather complex, and below we only give a summary of the results for the case of weak fields. We consider a magnetic field  $H$  along [001], i.e. in the  $z$  direction in the coordinate system of Fig. 1(c). The field is assumed to be weak in the sense that  $H \sim D$ . The presence of a field leads to changes in the spectrum, and we have found that quantitatively the most visible effect is related to the change of the  $b$  level energy.<sup>24</sup> In fact in magnetic field the  $b$  state mixes with the state  $|P_z\rangle$  (Eq. (9)), and the new eigenstate,  $c_1|b\rangle + c_2|P_z\rangle$ , has energy

$$E_b(H) = -\frac{1}{2} - \frac{3\sqrt{2}}{4}D - \frac{\sqrt{2}}{4}D \left[ 1 + \frac{16}{3} \frac{H^2}{D^2} \right]^{1/2}. \quad (24)$$

The on-site gap in a field,  $\Delta_H = E_b(H) - E_0$ , is plotted in Fig. 2(a) with a dashed line (for the specific choice  $H = 2D$ ). This behavior in turn enhances the tendency towards coplanar order, as evidenced by the dashed lines in Fig. 4(a,b). We do not present the exact form of the spin operators in this case, but just mention that they differ slightly from the zero-field case (22). In particular, at the coplanar point, the magnetic moments are not equal on all sites of the tetrahedron, as shown in Fig. 3(c), where the blue (upper) arrows are longer than the green (lower) ones.

## IV. CONCLUSIONS

In this work we showed that, in the anisotropic version of the pyrochlore lattice and in the presence of DM interactions,

two main types of spin order are possible, as summarized in Figure 3. These are (non-coplanar) chiral and coplanar orderings, depending on the sign of  $D$ . In our model the spin order also generally deviates slightly from the exact chiral and coplanar configurations, and this deviation itself depends on  $D$ . It is interesting to note that magnetic order of the kind described in this work was also found in the  $Sp(N)$  (large  $N$ ) approach to the Heisenberg pyrochlore model.<sup>25</sup> In addition, collinear order is also possible in that case, while DM interactions do not favor collinear states. The types of DM-induced order (chiral and coplanar) we found in the quantum case are also consistent with the Monte-Carlo results for the classical (3D) model.<sup>17</sup>

It is also important to emphasize that our approach assumes a specific type of lattice-symmetry breaking (as the explicit anisotropy of Fig. 1(b) demands.) In the full (3D) quantum pyrochlore lattice, with Heisenberg interactions only, it is believed that (spontaneous) lattice-symmetry breaking always takes place in the ground state,<sup>3,4,5,19</sup> and a certain dimerization pattern sets in. Two-dimensional projections previously studied<sup>11,12</sup> also exhibit valence-bond solid ground states. In our quasi-2D version (Fig. 1(b)), the dimerization tendency on the tetrahedra is very weak (as it occurs only in fourth order of perturbation theory) and does not interfere with the DM-induced magnetic order formation. At the same time our results are not directly relevant to the 3D pyrochlore lattice. Also, in this work we have not provided a dynamical mechanism for the layer decoupling, which we have taken as our starting point (the presence of spin-phonon interactions with the correct symmetry can certainly accomplish this task.) Instead, our goal has been the study of time-reversal symmetry breaking in certain anisotropic model situations with strong frustration.

Finally, the magnetic order sets in only below the Ising transition temperature  $T_c \sim J\Gamma^2$ , as dictated by the pseudospin interactions. Since  $\Gamma$  is determined by the DM interaction (Fig. 2(b)), we expect  $T_c$  to be small, and so are the magnetic moments (in all magnetic patterns),  $|\langle \mathbf{S}_i \rangle| \sim |\Gamma|$ . So far we are not aware of any convincing evidence that DM-induced order takes place in the pyrochlore-related compounds; nevertheless the presence of genuine antiferromagnetic order is a fundamental property of pyrochlore systems, which distinguishes them from other situations with more “trivial” manifestations of DM interactions (such as weak ferromagnetism.)

### Acknowledgments

We are grateful to M. Elhadj, F. Mila, A. Sandvik, M. Zhitomirsky, and A. H. Castro Neto for valuable discussions related to the topic of this paper.

### APPENDIX A: SPIN OPERATORS ON A TETRAHEDRON

For completeness we summarize the values of the various matrix elements used in the main text. At  $D = 0$ ,  $|s_1\rangle, |s_2\rangle$  are the singlet ground states, and  $|t_\alpha\rangle, |p_\alpha\rangle, |q_\alpha\rangle$ ,  $\alpha = x, y, z$  are

$S = 1$  states. The lower left (site) index on the spin operators corresponds to the upper sign on the right hand side (and the lower right index corresponds to the lower sign, if different.)

$$\begin{aligned}
S_{1,3}^\alpha &= -\frac{1}{\sqrt{6}} t_\alpha^\dagger s_1 \pm \frac{1}{2\sqrt{3}} p_\alpha^\dagger s_1 \mp \frac{1}{2} q_\alpha^\dagger s_2 + \text{h.c.} \\
&\quad -\frac{i}{4} e^{\alpha\beta\gamma} t_\beta^\dagger t_\gamma - \frac{i}{2} e^{\alpha\beta\gamma} q_\beta^\dagger q_\gamma \pm \frac{i}{2\sqrt{2}} e^{\alpha\beta\gamma} (t_\beta^\dagger p_\gamma + p_\beta^\dagger t_\gamma), \\
S_{2,4}^\alpha &= \frac{1}{\sqrt{6}} t_\alpha^\dagger s_1 \pm \frac{1}{2\sqrt{3}} q_\alpha^\dagger s_1 \mp \frac{1}{2} p_\alpha^\dagger s_2 + \text{h.c.} \\
&\quad -\frac{i}{4} e^{\alpha\beta\gamma} t_\beta^\dagger t_\gamma - \frac{i}{2} e^{\alpha\beta\gamma} p_\beta^\dagger p_\gamma \mp \frac{i}{2\sqrt{2}} e^{\alpha\beta\gamma} (t_\beta^\dagger q_\gamma + q_\beta^\dagger t_\gamma).
\end{aligned} \tag{A1}$$

The states are defined as

$$\begin{aligned}
|s_1\rangle &= \frac{1}{\sqrt{12}} [|\uparrow\downarrow\downarrow\uparrow\rangle + |\downarrow\uparrow\uparrow\downarrow\rangle + |\uparrow\uparrow\downarrow\downarrow\rangle + |\downarrow\downarrow\uparrow\uparrow\rangle \\
&\quad - 2(|\uparrow\downarrow\uparrow\downarrow\rangle + |\downarrow\uparrow\downarrow\uparrow\rangle)], \\
|s_2\rangle &= \frac{1}{2} [|\uparrow\downarrow\downarrow\uparrow\rangle + |\downarrow\uparrow\uparrow\downarrow\rangle - |\uparrow\uparrow\downarrow\downarrow\rangle - |\downarrow\downarrow\uparrow\uparrow\rangle], \\
|t_z\rangle &= \frac{1}{\sqrt{2}} [|\uparrow\downarrow\uparrow\downarrow\rangle - |\downarrow\uparrow\downarrow\uparrow\rangle], \\
|p_z\rangle &= \frac{1}{2} [|\uparrow\downarrow\downarrow\uparrow\rangle - |\downarrow\uparrow\uparrow\downarrow\rangle + |\uparrow\uparrow\downarrow\downarrow\rangle - |\downarrow\downarrow\uparrow\uparrow\rangle], \\
|q_z\rangle &= \frac{1}{2} [-|\uparrow\downarrow\downarrow\uparrow\rangle + |\downarrow\uparrow\uparrow\downarrow\rangle + |\uparrow\uparrow\downarrow\downarrow\rangle - |\downarrow\downarrow\uparrow\uparrow\rangle].
\end{aligned} \tag{A2}$$

Only the spin zero components of the triplets are shown, and in the notation of the type  $|\uparrow\downarrow\downarrow\uparrow\rangle$  the spins follow the order 1, 2, 3, 4, with the site labels defined in Fig. 1(c).

- 
- <sup>1</sup> R. Moessner and J. T. Chalker, Phys. Rev. Lett. **80**, 2929 (1998); B. Canals and C. Lacroix, Phys. Rev. Lett. **80**, 2933 (1998).  
<sup>2</sup> A. B. Harris, A. J. Berlinsky, and C. Bruder, J. Appl. Phys. **69**, 5200 (1991).  
<sup>3</sup> H. Tsunetsugu, Phys. Rev. B **65**, 024415 (2002).  
<sup>4</sup> E. Berg, E. Altman, and A. Auerbach, Phys. Rev. Lett. **90**, 147204 (2003).  
<sup>5</sup> R. Moessner, S. L. Sondhi, and M. O. Goerbig, Phys. Rev. B **73**, 094430 (2006).  
<sup>6</sup> S. Di Matteo, G. Jackeli, and N. B. Perkins, Phys. Rev. B **72**, 024431 (2005).  
<sup>7</sup> S. E. Palmer and J. T. Chalker, Phys. Rev. B **62**, 488 (2000).  
<sup>8</sup> O. Tchernyshyov, R. Moessner, and S. L. Sondhi, Phys. Rev. B **66**, 064403 (2002).  
<sup>9</sup> S. T. Bramwell and M. J. P. Gingras, Science **294**, 1495 (2001).  
<sup>10</sup> A. H. Castro Neto, P. Pujol, and E. Fradkin, Phys. Rev. B **74**, 024302 (2006).  
<sup>11</sup> J.-B. Fouet, M. Mambrini, P. Sindzingre, and C. Lhuillier, Phys. Rev. B **67**, 054411 (2003).  
<sup>12</sup> O. Tchernyshyov, H. Yao, and R. Moessner, Phys. Rev. B **69**, 212402 (2004).  
<sup>13</sup> O. A. Starykh, A. Furusaki, and L. Balents, Phys. Rev. B **72**, 094416 (2005).  
<sup>14</sup> M. Hermele, M. P. A. Fisher, and L. Balents, Phys. Rev. B **69**, 064404 (2004).  
<sup>15</sup> J. H. Kim and J. H. Han, arXiv:0807.2036.  
<sup>16</sup> I. Dzyaloshinsky, J. Phys. Chem. Solids **4**, 241 (1958); T. Moriya, Phys. Rev. **120**, 91 (1960).  
<sup>17</sup> M. Elhajal, B. Canals, R. Sunyer, and C. Lacroix, Phys. Rev. B **71**, 094420 (2005).  
<sup>18</sup> B. Canals, M. Elhajal, and C. Lacroix, arXiv:0807.0352.  
<sup>19</sup> V. N. Kotov, M. Elhajal, M. E. Zhitomirsky, and F. Mila, Phys. Rev. B **72**, 014421 (2005).  
<sup>20</sup> see, e.g., G. Chen and L. Balents, Phys. Rev. B **78**, 094403 (2008), and cited references.  
<sup>21</sup> X. G. Wen, F. Wilczek, and A. Zee, Phys. Rev. B **39**, 11413 (1989).  
<sup>22</sup> V. N. Kotov, M. E. Zhitomirsky, M. Elhajal, and F. Mila, Phys. Rev. B **70**, 214401 (2004).  
<sup>23</sup> S. Miyahara, J.-B. Fouet, S. R. Manmana, R. M. Noack, H. Mayaffre, I. Sheikin, C. Berthier, and F. Mila, Phys. Rev. B **75**, 184402 (2007).  
<sup>24</sup> The ground state energy (of the states  $|\Phi\rangle$  and  $|\Psi\rangle$ ) also changes in a field, but only by amount  $\sim D^2 H^2$ ,<sup>19</sup> which is much smaller than the field effect in (24).  
<sup>25</sup> O. Tchernyshyov, R. Moessner, and S. L. Sondhi, Europhys. Lett. **73**, 278 (2006).